Water Quality Co-effects of Greenhouse Gas Mitigation in US Agriculture

Subhrendu K. Pattanayak, Bruce A. McCarl, Allan J. Sommer, Brian C. Murray, Timothy Bondelid, Dhazn Gillig, and Benjamin DeAngelo[♣]

March 2004

Abstract

This study develops first-order estimates of water quality co-effects of terrestrial greenhouse gas (GHG) emission offset strategies in U.S. agriculture by linking a national level agricultural sector model (ASMGHG) to a national level water quality model (NWPCAM). The simulated policy scenario considers GHG mitigation incentive payments of $25 and $50 per tonne, carbon equivalent to landowners for reducing emissions or enhancing the sequestration of GHG through agricultural and land use practices. ASMGHG projects that these GHG price incentives could induce widespread conversion of agricultural to forested lands, along with alteration of tillage practices, crop mix on land remaining in agriculture, and livestock management. This study focuses on changes in cropland use and management. The results indicate that through agricultural cropland about 60 to 70 million tonnes of carbon equivalent (MMTCE) emissions can be mitigated annually in the U.S. These responses also lead to a 2% increase in aggregate national water quality, with substantial variation across regions. Such GHG mitigation activities are found to reduce annual nitrogen loadings into the Gulf of Mexico by up to one half of the reduction goals established by the national Watershed Nutrient Task Force for addressing the hypoxia problem.

♣ Senior authorship is not assigned. Corresponding author: Allan J. Sommer, Research Triangle Institute, P.O. Box 12194, Research Triangle Park, NC 27709, (919) 316-3993, sommer@rti.org fax: (919) 541-6683. Subhrendu Pattanayak, Allan Sommer, Brian C. Murray, and Tim Bondelid are with Research Triangle Institute. Bruce McCarl and Dhazn Gillig are with Texas A & M University. Benjamin DeAngelo is with the U.S. Environmental Protection Agency.

Water Quality Co-effects of Greenhouse Gas Mitigation in US Agriculture

1. Introduction

There is growing recognition that terrestrial activities in agriculture, land use change, and forestry can play an important role in reducing the potential impacts of climate change by mitigating greenhouse gas (GHG) emissions (Watson et al., 2000, McCarl and Schneider, 2000). A number of economic studies have focused on the cost of securing agricultural and forestry participation.[1] These studies estimate the costs of carbon sequestration by calculating the foregone agricultural returns that result from converting cultivated agricultural lands to forest, and the associated costs of conversion and management. However these studies have largely neglected the potential non-GHG environmental co-effects of GHG mitigation.

The Intergovernmental Panel on Climate Change (IPCC) Special Report on Land Use, Land-Use Change and Forestry suggests many land-use change and forestry (LUCF) practices for GHG mitigation would likely lead to broader environmental benefits such as improved water quality and quantity, reduced soil erosion and improved soil quality, greater biodiversity and reduced acidification, though there may be tradeoffs between GHG benefits and environmental quality in some cases (Watson et al., 2000). Recently, Matthews, O'Connor, and Plantinga (2002) have investigated the potential impacts on bird populations of GHG mitigation through the afforestation of croplands. While researchers have posited links between LUCF practices and water quality (Plantinga, 1996; Wear et al., 1998), little quantitative research exists on the water quality co-effects of land uses (Planting and Wu, 2003). Although a small but growing body of work (Atwood et al., 2000; Bansayat et al., 1999, 2000; Miller and Plantinga, 1999; Plantinga and Wu, 2003) has modeled changes in loadings (specifically reduced erosion, nitrogen and atrazine levels) from LUCF practices into water bodies, detailed assessments of in-stream water quality across the national hydrologic network have been lacking.

This study estimates the national and regional potential water quality co-effects from GHG mitigation in U.S. agriculture. Three inter-related features of our study distinguish it from past research on the environmental co-effects of LUCF practices. First, compared to most previous studies that have confined their analysis to a state, regional, watershed, or river level, we analyze the water quality impacts comprehensively, covering the 630,000 miles of rivers and streams that comprise the hydrologic network of the conterminous U.S.[2] Past studies have investigated the impacts of a carbon sequestration policy at the state level (Matthews, O'Connor, and Plantinga, 2002; Plantinga and Wu, 2003) However, state or regional analysis of the impacts of a GHG incentive program will not fully capture the costs or benefits of a national scale policy. Second, we model the decay, transport and fate of pollutants within this national hydrologic system, not simply the loadings at the 'contributing zone' (typically of erosion or a single pollutant e.g. nitrogen). The water quality modeling exercise explicitly accounts for baseline loadings and concentrations and, thereby, measures incremental impacts of LUCF practices for GHG mitigation. Because we model the transport and decay of pollutants, we can, for example, examine how LUCF practices in the US Corn Belt impacts water quality in the Gulf of Mexico. Third, we can develop a comprehensive index of water quality considering both in-stream toxics and nutrients, after accounting for their fate, transport and decay. Such an integrative index provides an overall measure of water quality at different levels of spatial aggregation.

From an economic perspective, quantitative estimates of co-effects can be important for designing GHG mitigation policies whether the goal is to determine if the total benefits of such policies outweigh the costs or, alternatively, to ensure that GHG policies do not generate negative co-effects. In an attempt to address these issues, this study develops first-order national estimates of water quality co-effects of terrestrial GHG mitigation strategies by linking a national level water quality model (NWPCAM) to a national level agricultural sector model (ASMGHG).

Terrestrial or biological carbon sequestration removes carbon dioxide (CO_2) from the atmosphere and stores it as carbon in biomass and soils. Typical land-use or land management practices that preserve and enhance terrestrial carbon storage include switching from conventional to low- or no-till agriculture, converting agricultural land to forests, protecting forests, lengthening rotation periods of the timber-harvest cycle, and establishing riparian buffers with forests or other native vegetation. Other forms of GHG mitigation from agriculture include management changes that induce reductions in nitrous oxide (N_2O) from fertilizer use and reductions in methane (CH_4) from livestock management.

The land-use and land management practices that sequester carbon and reduce GHG emissions have substantial overlap with practices that have historically been used to improve environmental quality by reducing farm-generated non-point source pollution. As such, widespread land-based GHG mitigation practices should, all else equal, simultaneously yield environmental **co-effects**. But economic behavior and market processes are complex. Feedback effects from GHG reduction incentives could induce secondary effects that diminish water quality (e.g., switching to crops with greater fertilizer requirements). So the net effect on water quality is an empirical issue requiring integrated modeling and quantitative analysis.

2. Model Components and Process Overview

Two national scale modeling systems were used to examine the joint GHG mitigation and water quality effects of carbon mitigation incentives in U.S. agriculture. This section provides a detailed description of the two component modeling systems and the technical approach developed to link the two.

2.1 Agricultural Sector Model with Greenhouse Gases (ASMGHG)

An agricultural sector model was used so that we could examine the complex market actions that would occur in the agriculture and forestry sector as a result of a GHG mitigation policy. For example, conversion of large acreages of agricultural lands to forestry would increase agricultural prices and reduce forest commodity prices, thereby providing economic incentives for some offsetting movement of land from forest to agriculture. The model used, ASMGHG, has been developed based on past work by McCarl and colleagues as reported in McCarl and Schneider (2000, 2001) and Chang et al. (1992). The version of ASMGHG developed by Schneider (2000) was expanded to include forestry possibilities for carbon production by including data on land diversion, carbon production, and the economic value of forest products as generated from a forestry sector model, FASOM (Adams et al., 1996) using 30-year average results over the 2000-2029 period.

ASMGHG depicts production, consumption, and international trade in 63 U.S. regions of 22 traditional and 3 biofuel crops, 29 animal products, and more than 60 processed agricultural products. ASMGHG simulates the market and trade equilibrium in agricultural markets of the U.S. and 28 major foreign trading partners. Domestic and foreign supply and demand conditions are considered, as are regional production conditions and resource endowments. The market equilibrium reveals commodity and factor prices, levels of domestic production, export and import quantities, GHG emissions management strategy adoption, resource usage, and environmental impact indicators. ASMGHG estimates several environmental impact measures including levels of greenhouse gas emission or absorption for carbon dioxide (CO_2), methane (CH_4), and nitrous oxide (N_2O); pollutant loadings of nitrogen (N) and phosphorous (P); and soil erosion. Pollutant and erosion outputs are calculated for each crop by management system based on a modified version of EPIC - the Erosion Productivity Impact Calculator (Sharpley and Williams, 1990).

In terms of GHG emission mitigation strategies, ASMGHG considers:

- Carbon sequestration from increases in soil organic matter (reduced tillage intensity and conversion of arable land to grassland) and from tree planting

- Carbon offsets from biofuel production (ethanol, power plant feedstock via production of switchgrass, poplar, and willow)
- Methane emissions from enteric fermentation, livestock manure, and rice cultivation
- Methane reductions from manure management changes
- Nitrous oxide emissions from fertilizer usage and livestock manure
- Direct carbon dioxide emissions from fossil fuel use (diesel, gasoline, natural gas, heating oil, liquefied petroleum gas) in tillage, harvesting, or irrigation water pumping as well as altered soil organic matter (cultivation of forested lands or grasslands)
- Indirect carbon dioxide emissions from fertilizer manufacturing
- Methane and nitrous oxide emission changes from biomass power plants

2.2 National Water Pollution Control Assessment Model (NWPCAM)

The National Water Pollution Control Assessment Model (NWPCAM; Little et al, 2003, RTI, 2000, 2001, Bondelid et al 1999, 2000, Bingham et al., 2000, Van Houtven et al 1999) is a national-scale modeling system designed to generate water quality estimates for two levels of spatial detail.[3] The first is a set of ~630,000 miles of rivers and streams, referred to as the RF1 level. The second level of detail is a much finer level created by disaggregating the RF1 layer into more than 3 million miles of rivers and streams and referred to as the RF3 system.[4] NWPCAM combines data on pollutant loadings with the RF1 or RF3 river network to create a spatially based surface water modeling framework which is capable of simulating transport, fate, and decay processes of nutrients and pollutants within the nation's waters. Specifically, NWPCAM uses the U.S. Geological Survey (USGS) conterminous United States Land Cover Characteristics (LCC) Data Set (Version 2). The LCC data set defines 26 land-use classifications that are defined at a one square kilometer (1 km^2) grid level. The land-use coverage is overlaid on the hydrologic routing framework to associate each land-use cell with a specific river reach, watershed, and hydroregion. Each land-use cell is assigned to the nearest routed reach for subsequent drainage area, stream discharge, and hydrologic routing purposes. Loadings from these land use cells are then assigned to their corresponding reach and routed through the national network via water quality modeling techniques.[5]

The method used for estimating non-point source loadings for both nutrients and conventional pollutants in NWPCAM is based on a network of export coefficients applied on a watershed level.[6] Export coefficients are empirical, aggregated parameters that describe the loading of a given nutrient or pollutant in terms of mass per unit time per unit area. The specification of export coefficients requires estimates of both the unit loading and the area of land within a catchment categorized into one of many land use and/or land cover types. Each land use type has its own unique export coefficient based on the land use classification and level of nutrients originating from the given land use.

NWPCAM models in-stream concentrations of nitrogen (N), phosphorous (P), and erosion or total suspended solids (TSS). Although erosion and TSS are not exactly the same, erosion is used as a proxy for TSS and will be referred to as such throughout the remaining discussion. Total suspended solids are used as a surrogate indicator of water transparency to characterize recreational service flows provided by a water body. Low TSS concentrations are associated with a high degree of water clarity. High concentrations of TSS are generally associated with murky or turbid waters and are therefore important contributors to perceptions of poor water quality. A simple net settling velocity was used to parameterize the interactions of particle size distributions with deposition and re-suspension. The revised universal soil loss equation (RUSLE) was used to amend the export coefficients used for TSS loadings on agricultural land-use cells (USDA, 1997). NWPCAM's nitrogen and phosphorous loadings were computed by land-use type and by ecoregion based on SPARROW (spatially referenced regression on watershed attributes; Alexander et al 2000, Alexander et al 2002), which is a statistical modeling approach for estimating major nutrient source loadings at a reach scale based on spatially referenced watershed attribute data.[7] This has the advantage of developing estimates of export coefficients that were spatially variable. In this study NWPCAM incorporates simplified first-order kinetics, in-stream modeling for the 630,000 mile (RF1) national stream network. Changes in loadings or land use as a result of proposed policies, regulations, or other environmental or social factors will result in a change in the export coefficients. NWPCAM models the national water quality impact of the changes.

Results from NWPCAM are presented using a water quality index (WQI) designed to incorporate the impact of the modeled pollutants on overall water quality. This index is based on past water quality valuation studies (McClelland 1974 and Vaughn 1986) and advancements in NWPCAM design. McClelland (1974) developed a continuous composite WQI index based on nine individual measures of water quality, including biological oxygen demand (BOD), dissolved oxygen (DO), fecal coliform bacteria (FCB), total suspended solids (TSS), nitrates (NO_3), phosphates (PO_4), temperature, turbidity, and pH. McClelland's index converts the concentrations of these water quality measures (milligrams per liter) into a corresponding score on a continuous scale ranging between 0 and 100. These scores were calculated by averaging the judgments from 142 water quality experts regarding the functional relationship between the conventional concentration measures and a 0-100 scale. Weights for each of the nine water quality characteristics were designed to sum to one and were again based on the judgments of the water quality experts. The scores and weights of the individual pollutant measures were combined in a multiplicative index of the following form:

$$\prod_{i=1}^{n} q_i^{wi} \qquad (1)$$

where q_i = water quality score ranging between 0 and 100 w_i = weight for each of the i water quality parameters; i = 1,2..n The index originally created by McClelland had to be modified for NWPCAM, which does not model temperature, turbidity, and pH. The re-weighted WQI contains six water quality parameters (n = 6 in equation 1) and translates NWPCAM output into a continuous WQI with values ranging between 0 and 100.[8] These WQI values can then be converted into beneficial-use attainment categories based on past work by McClelland 1974 and Vaughn 1986. These categories are discussed later in the results.

2. Model Process and Technical Approach for Evaluating GHG Policy Scenarios

To link GHG mitigation actions in agriculture to changes in water quality, we integrate changes in the ASMGHG environmental accounts for nitrogen (N), phosphorous (P), and erosion-total suspended solids (TSS) under alternative GHG prices as input to be used by NWPCAM. In turn, NWPCAM was used to estimate changes in the incidence of nitrogen (N), phosphorous (P), and total suspended solids (TSS) in the nation's waters along with estimates of changes in water quality. We compared "baseline" conditions (circa late 1990s) with two scenarios (circa 2020), which reflect agricultural reactions to two different prices for GHG mitigation ($25 and $50 per tonne of C equivalent), as reflected in ASMGHG outputs (e.g., land use and agricultural practices).[9] These hypothetical carbon prices were selected to represent values in the mid-range of prices typically evaluated for land-based GHG mitigation and not to find the optimal carbon price to reach a desired level of water quality improvement. Rather, this research is aimed at estimating the environmental benefits additional to the GHG emission reductions. An overview of the model system is presented in Figure 1 and discussed in detail below.

INSERT FIGURE 1

ASMGHG provides GHG scenario level data on changes in land-use, crop acreage and livestock holdings for 63 regions in the US.[10] While this is a fairly fine level of spatial detail for economic analysis, it is not sufficiently detailed for water quality modeling. Thus, additional spatial mapping was required to incorporate the results into NWPCAM. For N, P, and TSS loadings from cropland, ASMGHG results were further broken down to the county level using an auxiliary multiple objective programming model (Atwood et al 2000) which allocates the ASMGHG 63 region level crop mix changes to counties in a fashion most consistent with the USDA's Natural Resource Inventory (NRI) and Census of Agriculture observations on observed county level cropping patterns. In turn the county level loadings are mapped to the water system reaches defined in NWPCAM through the spatially defined 1 km^2 grid cells in the USGS LCC dataset.

Because ASMGHG and NWPCAM use different land use categorizations (USDA NRI and USGS LCC respectively), we build a cross-link to ensure that land use categories used in ASMGHG are reasonably mapped to the land use/cover categories used in NWPCAM.[11] The percentage change in loadings of the selected pollutants calculated in ASMGHG are processed in NWPCAM using procedures that account for NWPCAM's need to include every 1km^2 grid cell loading estimate, transport it to the nearest river reach, and then transport and decay the combined loadings (including for instance point sources) through the river network. The change in loadings calculated under the alternative GHG prices are then used in conjunction with the export coefficients in NWPCAM. [12]

There are seven major steps and associated sub-steps in this integration process (Figure 1). Each modeling step is described in turn below.

- Step 1. Set up the baseline versions of NWPCAM and ASMGHG. In these versions NWPCAM includes data on reach level animal manure loadings, municipal, industrial, and combined sewer overflow loadings, non agricultural non point source, non-manure-related, and agricultural NPS loadings. ASMGHG contains a depiction of production and resultant N, P and TSS.
- Step 2. Run ASMGHG under prices of $0 for baseline conditions, $25 and $50 per tonne carbon equivalent to simulate GHG mitigation incentives.
- Step 3. Disaggregate the ASM loadings data to a county level using Atwood et al (2000).
- Step 4: Disaggregate the ASMGHG county level data to generate percentage changes in N, P and TSS loadings on a NWPCAM reach level.
- Step 5 Run NWPCAM to compute baseline water quality indices.
- Step 6. Adjust the baseline NWPCAM agricultural non-point source data to reflect the percentage changes in cropland loadings from the ASMGHG GHG incentive scenarios.[13]

- Step 7. Run NWPCAM to derive changes in water quality indices due to the mitigation options selected in ASMGHG

3. Model Results

The outputs generated by integrating ASMGHG and NWPCAM are presented at the national and regional levels. The baseline conditions representative of the late 1990s (no GHG price) are first estimated in the models and then compared to the two alternative incentive scenarios, circa 2020. These two scenarios reflect the different prices for sequestered or released GHG's ($25 and $50 per tonne of C equivalent). The introduction of these price incentives causes ASMGHG to change its equilibrium allocation of land use, tillage, fertilization, crop mix and other management practices, commodity production and consumption, trade flows, and environmental loadings. The changes in environmental loadings are then transferred into NWPCAM to model the resulting changes in water quality.

The national level results generated by ASMGHG are presented in Table 1. Impacts of the two GHG prices are described in terms of three major categories: (1) economic welfare, (2) GHG's and, (3) environmental variables and land/use land cover. The key economic results generated by the GHG incentive payments (at both GHG price levels) are:

- **Production of traditional agricultural commodities declines.** Changes in management practices from the status quo to those induced by GHG incentives lead to an overall reduction in traditional agricultural commodities (crops and livestock). These reductions are partially offset by increases in non-traditional commodities (bio-fuel) and by forest plantations.
- **Agricultural prices rise.** The GHG policy-induced contraction in agricultural supply is only partly offset by an increase in imports. Together, this leads to a rise in the price of traditional agricultural commodities.
- **Consumer welfare falls.** The rise in agricultural prices causes consumers to pay more for food and other agricultural products, thereby reducing their well-being, all else equal.[14]
- **Agricultural producer welfare rises.** The economic effect of a rise in producer prices, along with the payments for GHG reductions outweighs any productivity losses from adopting the GHG mitigating practices. This causes the net income of farmers to rise relative to the base case.

- **Export earnings drop.** By adopting more expensive practices, US producers raise their costs relative to the rest of the world. This leads to a decline in US producers' share of world markets.

INSERT TABLE 1

Agricultural producers gain just over $900 million and $5.8 billion respectively under the low and high GHG price scenarios. Taking into account consumer losses, the total welfare costs of the incentive system would be about $1.1–1.2 billion. These costs need to be balanced against welfare gains in other parts of the economy in terms of reduced GHG damages, reduced mitigation costs in the nonagricultural sectors, and co-effects. However, those welfare gains are not estimated in this study.

Table 1 also shows total changes in net GHG emission resulting from the carbon pricing scenarios and agricultural practices. Within ASMGHG, greenhouse gas emissions and emission reductions for all major sources, sinks and offsets from agricultural activities for which data were available or could be generated are accounted for. As we will explain below, some of the GHG mitigation reported in Table 1 comes from activities for which corresponding water quality effects could not be estimated with the current modeling system. Consequently, the discussion further below will focus on the GHG effects from just those activities which can be directly tied to water quality changes. However, it is instructive to begin the discussion with this broader estimate of GHG mitigation from agriculture.

National net agricultural GHG emissions (gross emissions less changes in sequestration and biofuel offsets) decline from about 104.2 MMTCE per year in the baseline to 14.9 MMTCE per year under the lower carbon pricing scenario (a GHGE reduction benefit of 89.3 MMTCE/yr). At the high GHG price, agriculture becomes a net sink of –52.1 MMTCE/year (GHG mitigation of 156.3 MMTCE/year). The US Energy Information Administration (EIA) estimated the 1999 US GHG emissions to be 1,860 MMTCE (EIA 2002). The reduction in net emissions resulting from the $25 and $50 policy incentive could result in a 4.8% and 8.4% reduction in national emissions respectively. All species of GHG modeled (CO_2, CH_4 and N_20) are reduced by the incentive responses, but the effects are most dramatic for CO_2 with low- or no-tillage crop management occurring at the low price and biofuel offsets at the higher price.

The mitigation actions and environmental impacts resulting from the two GHG pricing scenarios are also presented in Table 1. The results suggest a drop in the amount of traditionally cropped agricultural land under both GHG prices. However, the number of cropped acres engaging in no till practices increases substantially under the carbon pricing scenarios. Finally, because forest is a more carbon-intensive land use than agriculture, the amount of agricultural land afforested increases by 5.8 and 12.5 million acres with the price incentives.

The modeled changes in these agriculture practices are the foundation of the water quality analysis, due to the resultant changes in loadings of nitrogen (N), phosphorous (P), and erosion or total suspended solids (TSS). The ASMGHG results show a decline in loadings for nitrogen and phosphorous at the low price scenario, and a reduction in all loadings at the higher GHG price. The most dramatic reduction in loadings is in TSS at the higher GHG price. Results reveal a potential reduction in TSS loading of over 252 million tonnes (7 percent).

Table 2 presents the changes in water quality at the national level and also at the disaggregated regional level. These WQI values are weighted averages of reach-specific values, with the stream mile per reach constituting the weights. That is, the WQI values in Table 2 are aggregated weighted averages and are not intended to suggest that all waters in the US or one of the sub-regions have the WQI reported.

INSERT TABLE 2

To place the WQI generated in NWPCAM in the context of the Clean Water Act, a WQI between 25 and 49 represents boatable waters, between 50 and 69 corresponds to fishable waters, and between 70 and 94 are swimmable.[15] From Table 2 we can see that the aggregate baseline water quality for the entire U.S. falls in the upper range of fishable, nearly reaching swimmable levels. This is, in some sense, a measure of average water quality nationwide. The reductions in loadings that result from the GHG mitigation activities increase the national aggregate average water quality 1.38 points (about 2 percent) on a 1 to 100 scale. These improvements move the aggregate water quality measure into the swimmable range.

The map presented in Figure 2 corresponds to the $25/tonne scenario and visually summarizes the information presented in Table 2. The unit of change presented in the maps is the change in the WQI from the baseline conditions. The reductions in water quality (–40 to –1) represent the bottom 5 percent of all changes in water quality in the country.[16] The remaining reaches are broken down into three additional categories; no change (0), a positive improvement (1–5) (90% of all changes in water quality fall within these middle ranges 0 and 1-5), and the top 5 percent of all reach-level improvements in the country (6-100).[17]

An interesting result revealed in Table 2 is that, the average improvement in water quality on the national scale is of the same magnitude for both levels of CE prices. Within the limited set of model runs we performed, these results offer some evidence of potential diminishing returns to water quality improvements.[18] We will return to this issue in the discussion section. Regional differences in WQI changes can also explain this result to some extent. Some regions show a larger improvement in water quality under the smaller GHG price than the higher price, while the opposite is true in other regions.

INSERT FIGURE 2

National level aggregation masks the results that occur within the country. To investigate this phenomenon we look at the regional breakouts of the two GHG pricing scenarios. The regional results for the farmland impacts of GHG pricing are aggregated from the original 63 ASMGHG regions into the 10 broader regions first presented in Table 2 and defined in Table 3. We use these regional definitions to disaggregate our results.

INSERT TABLE 3

Table 4 presents GHG mitigation on cropland by each region under baseline and two GHG incentive prices ($25 and $50 per tonne). It is important to note that the GHG mitigation estimates in Table 4 are only for the changes in cropland practices associated with the water quality changes modeled here. Therefore the national GHG total in Table 4 is a subset of the national total in Table 1, because Table 1 includes the GHG mitigation from afforestation and livestock practices for which we were not able to estimate water quality impacts.

The two regions producing the largest GHG reductions are the Corn Belt and Lake States. The Corn Belt, which is heavily dominated by agriculture, reports the largest absolute GHG reduction at over 27 MMTCE. Much of the GHG mitigation in this region is attributable to the adoption of conservation tillage practices. The Lakes States report the second largest reduction in GHG. This result is not surprising based on the comparatively low costs of carbon sequestration in this region resulting from readily available marginal croplands and high rates of carbon accumulation in the region specific forest characteristics (Adams et al. 1999, Plantinga Mauldin and Miller 1999).

INSERT TABLE 4

Table 5 presents the changes in N, P, and TSS cropland loadings resulting from the land use and agricultural management changes. There are two discernible patterns in these results. First, the largest change in loadings is for TSS where there is considerable regional heterogeneity among the level of loadings. In addition to the loading differences among regions, there is also some significant heterogeneity for TSS at the two GHG prices. For example, the Southeast, Northeast, and North Plains regions generate increased loadings of TSS at the low price, but substantially reduce loadings at the higher price. However, the opposite pattern is reported for the Appalachian region. These stark inter-regional differences are not found in N and P. The divergent patterns reflect the complex relationship between GHG incentives, changes in practices, crop mix and aggregate pollutant loadings.

INSERT TABLE 5

Second, while there is evidence of regional heterogeneity in the changes in N and P loadings associated with GHG mitigation, the overall changes are relatively small. All of the regions show a small reduction or no change in the loadings of these pollutants from the baseline conditions at the low price. The heterogeneity is more easily identified at the higher price where some of the regions that initially had no change in the baseline loadings show a slight reduction and, in some cases, an increase. For example, the Southeast and North Plains regions show no change from the baseline loadings of nitrogen at the low price. However, the higher GHG price reveals that the Southeast exhibits a reduction in nitrogen loadings while the North Plains shows an increase. Again, these are relatively small changes from the baseline conditions.

Recall from Table 2 the weighted regional water quality indexes calculated by NWPCAM. The majority of the improvements are occurring in five of the regions across the U.S., all of which improve by 2.5 WQI points or more. The North Plains region had the lowest baseline WQI and realizes the largest improvement (8 percent) from land use transitions and reductions in loadings as modeled by ASMGHG. The South Plains, Lake States, Corn Belt, and Delta States exhibit regional WQI increases of over three percent to round out the top 5 regions with the largest improvements in water quality. These areas of improved WQI can clearly be identified in Figure 3. These five regions show the largest collection of blue river reaches, or improvements in the WQI from the baseline conditions.

There is an interesting phenomenon that occurs with the WQI under the two GHG prices. All of the regions show an improvement in water quality under the initial GHG pricing scenario. However, under the higher price scenario, the *changes* from the baseline conditions are about the same as at the lower GHG price. This occurs because of an increased diversion of land from traditional cropping to trees and biofuels, which creates land scarcity in traditional agriculture and induces some intensification of cropping (and resulting loadings) on the remaining crop lands. Although there are still improvements under the higher GHG price, the results suggest that increased GHG mitigation may produce increased water quality improvements at a diminishing rate, at least for the prices investigated here. Without evaluating a wider range of carbon prices (e.g. $2 - $200) however, it would be premature to deduce that the results presented here suggest positive but diminishing benefits from all GHG mitigation efforts on cropland. Recall from Table 1 that GHG mitigation on cropland is not substantially higher at the higher price either.

This regional analysis also allows us comment on the hypoxia problems in the Gulf of Mexico. Hypoxia is a condition of low levels of dissolved oxygen in a water body. This condition is caused by increased levels of nutrients such as N and P in tributary waters. These nutrients often originate from increased agricultural run-off due to the loss of streamside wetlands and vegetation (Goolsby et al., 2000). According to the 1997 Mississippi River/Gulf of Mexico Watershed Nutrient Task Force, an important step in solving the hypoxia problem lies in reducing the hypoxic zone in the gulf to be less than 5,000 square kilometers by the year 2015. To achieve this goal it was estimated that the annual nitrogen loadings to the Gulf of approximately 1.5 million tonnes, especially nitrates, would need to be reduced by 20 to 30 percent (Greenhalgh and Faeth, 2001).

Table 6 reports changes in N loadings to the Gulf of Mexico. Under the two pricing scenarios, NWPCAM results show potential nitrogen reductions of up to 144,000 and 160,000 tonnes per year, respectively.[19]

Converting the loadings to equivalent units of measure (1 metric tonne = 1.1022 short tons,) reveals that the reductions in nitrogen loadings resulting from the portfolio of GHG mitigation activities could play a role in addressing the hypoxia problem. The predicted changes in management and associated pollutant loadings could account for up to an 8.7 and 9.7 percent reduction in annual loadings to the Gulf, or nearly one half to one-third of the reduction goals established by the Watershed Nutrient Task Force in 1997.

INSERT TABLE 6

4. Conclusions

By linking an agricultural sector model with a national water quality model, we provide simultaneous estimates of GHG mitigation, sectoral response, regional production, and associated water quality co-effects under GHG mitigation incentives. These results only cover a subset of land use activities (namely agriculture) and water pollutants, yet they suggest that GHG mitigation activities in agriculture can, on balance, generate water quality co-effects, rather than co-costs. Figure 2 illustrated the nationwide changes in water quality resulting from the GHG pricing scenarios. The map for the change in WQI under the GHG incentives provides much more “texture” as to where water quality changes are occurring than can be shown by tables or graphs. The key water quality results are as follows:

- Nationwide water quality increased 1.38 water quality index points (~2%) under both GHG pricing scenarios. Water quality improves in every aggregate region in the country, although the level of improvement varies under the pricing scenarios.[20]
- Five regions, all roughly East of the 100th meridian (North Plains, South Plains, Lake States, Corn Belt and the Delta States) experienced the largest water quality improvements ranging from about 3 to 8 percent.
- Nitrogen loadings into the Gulf of Mexico could be reduced by over 9 percent, roughly one third to one half of the total reduction recommended by the Watershed Nutrient Task Force goals.

As Tables 2 and 3 and Figure 2 illustrate, there is considerable heterogeneity across regions and GHG incentive scenarios in terms of agricultural loadings and in-stream water quality. These heterogeneous results reflect at least two complicating factors. First, variations in regional comparative advantage in agricultural production and GHG mitigation cause inter-regional shifts in production activities in response to the GHG incentives. This reflects the spatial and cross-sectoral equilibrium aspects of the ASMGHG economic model. The model allows prices of agricultural commodities to increase as agricultural supply falls because of the change in management practices and conversion of marginal croplands to forest. In some circumstances (e.g., Appalachia under the higher GHG price scenario), the indirect response caused by these agricultural price effects may more than offset management responses due to GHG incentives, thereby leading to a net increase in the loadings of some pollutants. Second, some activities that enhance GHG benefits have some offsetting water quality costs. For example, runoff may increase on converted lands, or greater infiltration of water into soils may occur as the result of increased organic matter and water-holding capacity over time potentially increasing nitrate infiltration into ground water.

It is possible for pollutant loadings to increase with the GHG incentives. Recognize that establishment of a carbon price is a GHG incentive, not a loadings or water quality incentive. This incentive causes agricultural practices to change in ways that mitigate/conserve GHGs. In the case of conservation tillage, the synergy is seemingly positive (more carbon in the soil, less erosion (TSS), and perhaps less N, P needed). However, it is also possible that carbon prices cause farmers to intensify input use or switch to crops with higher nutrient requirements and therefore higher runoff. So, on balance, we find positive co-effects, but this is an empirical finding, not a universal article of truth.

We also find that going from the lower to the higher GHG price did not substantially improve water quality, potential evidence of diminishing returns over the price range considered ($25 -

$50 per tonne). That is, while the initial GHG reduction results in a material improvement in the WQI, the larger GHG price improves water quality, but to a lesser degree than the initial impacts. Consider five explanations. First, the direct GHG mitigation effects diminish as we move from the lower to the higher GHG price, so it is not too surprising that the water quality effects are diminishing as well. Second, as mentioned earlier, the actual commodity being purchased is a reduction in GHG, not water quality improvements. The water quality improvements are a by-product or added benefit resulting from the proposed policy actions of establishing a carbon market. Third, agricultural lands (linked to ASMGHG) are just one from a myriad set of point and non-point source loadings into the nation's waters; therefore, the GHG mitigation activities in our analysis can only affect a fraction of total loadings. Fourth, as the GHG incentive price rises, more land is diverted from traditional agricultural production to biofuels, forests, and grasslands. The remaining crop land is farmed more intensively with increased inputs and this tends to moderate the water quality gains. Fifth, we have not considered the entire price range - significantly lower (e.g. $2) or higher ($200) prices might have showed significant changes. That is, notwithstanding the previous four explanations, it also possible that there are model or process (economic or ecological) rigidities, and we simply did not find those thresholds.

It is critical to review some qualifications to the analysis and results presented in this report. Perhaps the biggest temptation is to view Figure 2 as a source of microscopic or reach specific detail. We must recognize the inherent traits of models such as ASMGHG and NWPCAM that are built on micro-level elements or cells. Projections and output from these aggregated models are more accurate at the aggregate level than at the individual cell. This is because the macro models are relying in a sense on the "law of large numbers." In other words, we can assume that there is a fair degree of random error at the individual reach level, but the pluses and minuses cancel, so that regional averages are roughly correct. As such, the modeling exercise is best viewed as providing first-order geographically aggregated estimates of policy-induced GHG and water quality changes.

Additionally, there are factors outside these model results that may have important environmental consequences. For example, increased carbon stocks, conversion of croplands to grassland and increased reliance on biofuels are some of the inherent results of the changes in the management of agricultural lands with the new GHG prices. These actions and associated results may increase long run soil productivity as they may increase its ability to retain nutrients and moisture, thus reducing the reliance on fertilizers and increasing its resistance to drought by reducing water requirements. Moreover, changes in land use and land management can alter the biodiversity of the landscape's flora and fauna. The potential for these additional co-effects are important factors to be considered in future analyses.

Although the study was successful in accomplishing its primary objectives, two areas warrant further attention in future research. First, it could be critical to evaluate how loadings from livestock manure and afforestation influence the overall water quality results. Second, it would be informative to monetize the co-effects through benefits transfer methods, as in Plantinga and Wu (2003) or using monetary estimates reported in Carson and Mitchell (1993). Such monetized estimates would allow us to evaluate whether the benefits of water quality improvements sufficiently supplement GHG mitigation benefits to offset, or possibly outweigh, the cost of carbon payments.

Acknowledgments

Support for this research came from the US Environmental Protection Agency (USEPA), Office of Atmospheric Programs, USEPA Office of Water, and USEPA/NSF Science to Achieve Results (STAR) grant, and from Research Triangle Institute. However, these reflect the author's views, not necessarily the positions of the sponsoring institutions. The authors are grateful to seminar participants at the Forestry and Agriculture Greenhouse Gas Modeling Forum, Ken Andrasko, John Powers, Mahesh Podar, Suzie Greenhalgh, and three anonymous reviewers for their comments.

Appendix A NWPCAM Model Overview

NWPCAM is a steady state mathematical model that simulates levels and changes in water quality resulting from changes in point and non-point source pollutant loadings into the surface water system of the conterminous U.S. The model simulations incorporate such key features as stream flow, the input of point and non-point sources of pollutants, and the principal interactions of the constituents selected as state variables for their relevance to the key water quality issues. The water quality model is constructed by coupling theoretical equations that describe the various mechanisms affecting the behavior of the key water quality indicators. NWPCAM incorporates the key processes and interactions for each of the following topics in discrete model components:

- Temporal and spatial dimensions
- Physical domain and transport processes
- Stream flow and channel geometry
- Point and non-point source loads
- Water quality kinetics
- Model performance measures
- Water quality index (ladder)

NWPCAM 1.1 performs both national- and watershed-level modeling of conventional pollutants in the major inland rivers and streams, larger lakes and reservoirs, and some estuarine waters in the lower 48 states of the U.S.[21] To simulate the levels of the water quality indicators, NWPCAM models the following instream parameters:

- dissolved oxygen concentration (DO)
- dissolved oxygen saturation
- percent dissolved oxygen saturation
- dissolved oxygen deficit
- fecal coliform (FC)
- total suspended solids (TSS)
- 5-day biochemical oxygen demand (BOD_5)
- Ultimate biochemical oxygen demand (BOD_U)
- Total Kjeldahl nitrogen (TKN)

The current NWPCAM framework is intended to capture a national-scale "snapshot" of water quality conditions resulting from the simulation of baseline conditions and different policy scenarios, and thus requires a much coarser spatial scale than that needed for a detailed model of individual watersheds.

A.1 Key Model Dimensions

A.1.1 Conservation of Mass Principle

The model framework for NWPCAM is based on the principle of conservation of mass. The mass balance principle holds that all inputs and outputs of mass in a stream, river, lake, or estuary must be accounted for over a "control volume" of the waterbody. Within a reach of a river, physical inputs of material include the amount of mass brought into a reach by upstream boundary inflows, tributaries, and point and nonpoint source inputs from the watershed. Physical outputs of material from a reach include the amount of mass leaving a reach by stream flow across a downstream boundary. Within a reach of a river, additional inputs (sources) and outputs (sinks) of material are influenced by physical, biological, and geochemical kinetic processes. The form of the conservation of mass principle over a control volume (e.g., reach of a river) is expressed here as:

Rate of mass change in volume = Rate of mass entering volume
- Rate of mass leaving volume
+ Rate of mass produced in volume
- Rate of mass lost from volume

A.1.2 Temporal Resolution
As a steady-state model using the stream and river summer flow, temporal fluctuations in pollutant loads, stream flow, and ambient water quality conditions, occurring at higher frequencies (i.e., hours, days, weeks, months) than the much lower seasonal (summer) frequency, are not represented in NWPCAM. Observed stream flow and ambient water quality data used in the steady-state model are based on data extracted for the summer months (July-September) to generate summary statistics as input data for the model. In contrast to stream flow and ambient water quality, municipal and industrial effluent loading data typically do not vary significantly during the course of a year. Effluent flow and pollutant loading data extracted from EPA databases for all months (circa 1995) were assigned as annual mean values for input to the model. As a consequence of winter-summer seasonality in precipitation and runoff, nonpoint source loading of pollutants vary significantly on a seasonal basis. However using the annual mean values for nonpoint loadings, much of the intra-annual variation is not captured in NWPCAM.

A.1.3 Spatial Resolution
The concentrations of water quality constituents can vary in three dimensions within natural waters. However, for simplicity a one-dimensional (1-D) (laterally and vertically invariant) spatial representation was adopted for this framework. In NWPCAM, the distributions of water quality constituents are spatially referenced to a 1-D longitudinal coordinate system measured as river miles along the transport path length of a river. The origin (river mile = 0) of the 1-D coordinate system is defined as the location of the river system where the river ultimately discharges into large, open waters (e.g, Gulf of Mexico, Atlantic Ocean, Pacific Ocean, Chesapeake Bay, Lake Michigan).

EPA's RF1 database is used as the foundation of the physical domain in NWPCAM to describe the connectivity network designed to efficiently route flow and pollutant loads coalescing from headwater streams to tributaries to large rivers. Within the continental United States, RF1, accounts for 632,552 miles of rivers in approximately 68,000 reaches (of which 61,000 are in the flow path, e.g., not shoreline). The mean length of an RF1 reach is about 10 miles with a drainage area of about 114 mi^2. The density of the streams and rivers included in RF1, was selected, in part, to ensure that the discharge locations of most of the municipal and industrial wastewater treatment plants included in the National Pollution Discharge Elimination System (NPDES) database were accurately represented in the Reach File database.

A.2 Water Quality Model Framework
Monitoring data have been used in NWPCAM as a source of input data, and to validate and calibrate the model. For example, as an input to the model, data from the PCS and NEEDS Survey databases provide point source loadings data, while USGS gauging station data provide stream flow and velocity data. Monitoring data are also used in calibrating and validating the model. These data are used as a benchmark for evaluating model performance.

A.2.1 Stream Flow and Channel Geometry
Under the assumption of steady-state flow and 1-D transport in free-flowing streams and rivers, geometry (depth, width, cross-sectional area, and wetted perimeter) for each RF1 reach are estimated using the mean summer flows and velocity data estimated for each RF1 reach and the

"stable channel analysis" developed by the U.S. Bureau of Reclamation (Henderson, 1966). A reach is represented in the stable channel analysis with a 35-degree side slope trapezoidal cross section with mean channel depth, channel depth at the center of the reach, cross sectional area, wetted perimeter, and velocity assumed uniform over the downstream length of the laterally and depth-averaged RF1 reach. The stable channel analysis, based on bed shear and local depth, provides a methodology to estimate the mean depth and wetted perimeter of a reach as a function of reach cross-sectional area. Using the mean and low flow conditions reported by Gate's (1982) and velocity data assigned to each RF1 reach, the cross-sectional area and mean depth in the reach were estimated from summer mean stream flow and velocity.

A.2.2 Point Source and Nonpoint Source Loads

The approach used in NWPCAM for estimating nonpoint source loadings for both nutrients and conventional pollutants is based on an export coefficient model that is applied on a watershed level. Export coefficients are empirical aggregated parameters that describe the loading of a given nutrient or pollutant from a specific land use category in terms of mass per unit time per unit area. The specification of export coefficients requires estimates of both the unit loading and the area of land within a catchment described in terms of different types or classes of land use and/or land cover.

A.2.2.1 Point Source Loads

Point sources represented in NWPCAM include municipal and industrial wastewater treatment plants and combined sewer overflows. Pollutant discharges, obtained from the monitoring data described above, from municipal and industrial outfall pipes are represented in the model by estimates of annual mean loading rates input at a discrete location along the length of a stream or river. Pollutant discharges from urban runoff and combined sewer overflows, accounted for by an urban network of multiple discrete outfall pipes discharging to one or more waterways, are aggregated and distributed uniformly to RF1 reaches within the urban land use portions of a watershed (see below). Pollutant loads for point sources are estimated for each of the following state variables selected for NWPCAM: 5-day biochemical oxygen demand (BOD5), Total Kjedhal nitrogen (TKN), Dissolved oxygen (DO), Total suspended solids (TSS) and Fecal coliform bacteria (FCB)

Urban Runoff and Combined Sewer Overflows

The public works infrastructure in every town and city includes an urban stormwater drainage system designed to collect and convey runoff from rainstorms and snow melt. Many older cities have urban drainage systems that convey both stormwater runoff and raw sewage. The urban runoff and CSO loadings are included in the NWPCAM modeling framework and are based on data obtained from Lovejoy (1989) and Lovejoy and Dunkelberg (1990).

A.2.2.2 Nonpoint Source Loads

Nonpoint source loads, characterized as intermittent diffuse inputs distributed over an entire drainage basin, are related to hydrologic conditions, topography, physiography, and land uses of a watershed. In NWPCAM, pollutant loads for non-point sources were computed by land-use type by ecoregion based on SPARROW (*SPA*tially *R*eferenced *R*egression *O*n *W*atershed attributes; Alexander et al 2000, Alexander et al 2002) which is a statistical modeling approach for estimating major nutrient source loadings at a reach scale based on spatially referenced watershed attribute data.[22] An optimization algorithm was developed to estimate non-manure loadings by comparing SPARROW non-manure non-point source estimates for cataloging units with modeled outputs. The optimal coefficient set was determined for both nitrogen and phosphorus for each ecoregion within a hydroregion. This was accomplished by iteratively running an optimization routine using a genetic algorithm to estimate loading coefficients for major land use categories present in the ecoregion. Non-point sources were delivered directly to the RF1 reaches for hydrologic routing through the river/stream network.

A.2.3 Water Quality Kinetics

Each of the pollutants modeled in NWPCAM behaves differently, and must be modeled accordingly. For example fecal coliform bacteria have a mortality rate that differs under various water quality conditions. However with constituents such as TSS, there is no mortality rate, rather a settling loss phenomena occurs and must be modeled. For all constituents included in NWPCAM, the model methodology accounts for the following phenomena (if it pertains to the specific pollutant) through detailed mathematical calculations:

- Calculation of the Upstream Boundary
- Rates of Oxidation/Decomposition/Reaeration/Mortality
- Settling Loss
- Removal Rate

A.2.4 Dissolved Oxygen

Dissolved Oxygen (DO) is included in the model as a surrogate indicator for aquatic health. High levels of oxygen are characteristic of good water quality conditions that can support a high-quality fishery and a high diversity of aquatic biota. NWPCAM assumes that oxygen production from photosynthesis (P) and oxygen consumption from respiration (R) balance to a net production of zero (i.e., P = R and P - R = 0). In NWPCAM, the contribution of oxygen from atmospheric re-aeration is accounted for by water temperature, velocity, and depth of the river channel.

A.2.5 Ultimate Carbonaceous Biochemical Oxygen Demand

Organic carbon is represented in the NWPCAM framework by the ultimate carbonaceous component of biochemical oxygen demand (CBODU). CBODU, a measure of the oxygen equivalent needed to completely decompose oxidizable organic carbon in wastewater effluent and surface waters. Labile/refractory and dissolved/particulate fractions of total organic carbon are not differentiated in NWPCAM. The first-order decomposition rate assigned to describe the decay of organic carbon thus represents a composite of slow (refractory) and fast (labile) decay rates. The in-stream removal of particulate organic matter is represented with a second loss term to account for settling of the particulate fraction of organic carbon. As treatment levels increase, particulate organic matter in the effluent is expected to be reduced to the extent that the in-stream BOD removal rate via settling is lowered to approach the in-stream decomposition rate. Differentiation of the rates of decomposition and settling removal loss is essential for NWPCAM to account for different treatment levels. The total loss rate of organic carbon (as CBODU) from the water column is determined by the sum of the loss due to decomposition and the loss due to settling out of particulate organic matter. Since the relative loss due to settling is greater in shallow waters, particularly in streams less than approximately 1 meter in depth, a depth-dependent formulation for the removal rate is used in the model (Bowie et al., 1985; Hydroscience, 1971; 1972). External loading of CBODU is represented as inputs to each RF1 reach of a catalog unit by municipal and industrial point source dischargers, urban runoff, CSOs, and rural runoff.

A.2.6 Total Kjedhal Nitrogen

Nitrogen is composed of both inorganic and organic forms with ammonia, nitrite, and nitrate being the inorganic constituents. In NWPCAM the impact of nitrification on oxygen consumption is the component of the nitrogen cycle that is the most relevant for the design of the simplified Version model. TKN is defined as a state variable in NWPCAM to account for the nitrogenous component of the BOD demand (NBOD). Using the stoichiometric ratio for oxygen:nitrogen (4.57 grams O_2 per grams of N), the loss of TKN via nitrification defines the equivalent oxygen loss in the model balance formulation for oxygen.

Source terms for the oxidizable nitrogen submodel include external loads accounted for by municipal and industrial discharges, CSOs, and urban and rural runoff. In the absence of a national database to characterize benthic regeneration rates for ammonia, the stoichiometry for oxygen:nitrogen of 15.1:1 by weight (Redfield et al., 1963) is used to define the equivalent amount of ammonia nitrogen released by decomposition of organic carbon in the sediment bed. The benthic release of ammonia to the overlying water column is estimated from the reachdependent parameter values assigned for sediment oxygen demand (Di Toro, 1986; Di Toro et al., 1990).

A.2.7 Total Suspended Solids

In NWPCAM, suspended solids are used as a simplified surrogate indicator of water transparency as a recreational component to characterize beneficial uses of a waterbody. Low suspended solids are characteristic of a high degree of water clarity in contrast to high concentrations of suspended solids that are correlated to murky, turbid waters.

The submodel component of NWPCAM for suspended solids functions in such a way that the complex sediment transport interactions of particle size distributions with deposition and resuspension are parameterized by a simple net settling velocity. With this assumption, no distinction is made in the model regarding the relative fractions of cohesive (clays and silts) and noncohesive (sands) particle sizes.

A.2.8 Fecal Coliform Bacteria

In NWPCAM, FCB is used as a proxy for the risk of exposure to waterborne diseases as the public health component to characterize beneficial uses of a waterbody. Low densities of FCB are characteristic of a low public health risk of exposure for waterborne diseases. The submodel in NWPCAM for FCB is simplified in that the components of the mortality and net settling loss rate for FCB are parameterized by a simple temperature-dependent aggregate net loss rate.

A.2.9 Estimating Mean Summer Streamflows and Velocities

The RF1 data contains paired values of flow and velocity for mean annual and low flow (~7-day-10-year) conditions. As explained above, the condition used in NWPCAM for is a mean summer flow (July-September). The USGS stream gauges in the Hydro-Climatic Data Network (HCDN) were selected to estimate mean summer flows. These gauges most accurately represent relatively natural hydrologic conditions as they are not influenced by controlled releases from reservoirs. For each HCDN gauge, the ratio of the mean summer flow to mean annual flow is computed. These ratios are then grouped across each ecoregion, and a mean is calculated. The result of this process is an ecoregion-level multiplier that is then applied to each cataloging unit that is represented by the dominate ecoregion within the unit.

The methodology for assigning reach dependent flow and velocity is done on a reach basis, using the paired low flow-velocity and mean flow-velocity values to develop reach-specific coefficients. Since, for each RF1 reach, there are paired values for flow and velocity. When the model is run under a summer flow condition, a corresponding summer velocity is computed by reach.

A.2.10 Land Use information

Mentioned earlier, pollutant loadings from the different land use types assigned to specific RF1 reach. The basis for the land-use/land-cover spatial coverage used by NWPCAM is the U.S. Geological Survey (USGS) conterminous United States Land Cover Characteristics (LCC) Data Set (Version 2). The LCC data set defines 26 land-use classifications. Land-use/land-cover data are defined at a square kilometer cell grid level in the LCC.

Each land-use cell is overlayed on counties as well as assigned to the nearest routed RF1 reach for subsequent drainage area, stream discharge, and hydrologic routing purposes. The USGS developed the LCC data set by classifying 1990 NOAA Advanced Very High Resolution Radiometer (AVHRR) satellite time-series images. Post-classification refinement was based on other data sets, including topography, climate, soils, and eco-regions (Eidenshink, 1992). The LCC data set is intended to offer flexibility in tailoring data to specific requirements for regional land-cover information.

A.2.10.1 Integrating Land-Use Cells and RF1

The image used to assign land-cover cells to an RF1 reach has a pixel size of 8-bit (1 byte), representing an area of 1 km^2. The image contains 2,889 lines and 4,587 samples covering the entire conterminous United States. Based on this information, it is possible to extract a specific area from the image into an ASCII file using a C-computing language routine. This approach allows for importing only portions of the image, thereby reducing loading and processing time considerably compared to a full-image import with a commercial GIS package. The ASCII file then is used to generate a point coverage in ARC/INFO, which is converted to geographic coordinates to process it with existing RF1 reach coverages.

Resolution of the land-use coverage data set is a square kilometer. The coverage for the continental United States comprises approximately 7,686,100 land-use cells at the square kilometer cell grid scale. The land-use coverage is overlaid on the RF1 hydrologic routing framework to associate each land-use cell with a specific RF1 reach. Each land-use cell is assigned to the nearest routed RF1 reach for pollutant loadings, subsequent drainage area, stream discharge, and hydrologic routing purposes. Information in the land-use/land-cover database includes the land-use/land-cover code for each cell, the watershed (HUC) code and county code in which the cell is located, the RF1 reach associated with the cell, and related information. On a hydroregion basis, each land-use/land-cover cell is given a unique identification number for modeling purposes

A.3 Changing Loadings for Policy Analysis

The default conditions of the model input that define “Baseline” conditions are loadings based on circa 1990s data as derived from EPA, and other, databases. Alternative scenarios operate on the baseline loadings, either increasing or decreasing certain loadings, depending on the scenario. For the purposes of the paper presented here, the policy scenario is the presence of a carbon trading market. The resulting changes in land use and forestry create associated changes in the in pollutant loadings. Estimates of industrial loadings are left unchanged in the policy scenario.

References

Adams, R., Adams, D., Callaway, J., Chang, C., McCarl, B. 1993. Sequestering carbon on agricultural land: social cost and impacts on timber markets. *Contemporary Policy Issues XI*, 76–87.

Adams, D.M., R.D. Alig, B.A. McCarl, J.M. Callaway, and S.M. Winnett. 1996. The Forest and Agricultural Sector Optimization Model: Model Structure and Applications. USDA FS Research Paper PNW-RP-495, Portland, Oregon.

Alexander, R.B., Johnes, P.J., Boyer, E.W., and Smith, R.A. 2002. A comparison of models for estimating the riverine export of nitrogen from large watersheds. *Biogeochemistry*, 57/58, 295-339.

Alexander, R.B., Smith, R.A., and Scwarz, G.E. 2000. Effect of stream channel size on the delivery of nitrogen to the Gulf of Mexico. *Nature* 403. 758-761

Alig, R., D. Adams, B. McCarl, J. Callaway, S. Winnett. 1997. Assessing the Effects of Global Change Mitigation Strategies with an Inter-temporal model of the U.S. Forest and Agricultural Sectors. *Environmental and Resource Economics*. 9:259-274

Atwood, J.D., B.A. McCarl, C.C. Chen, B.R. Eddleman, R. Srinivasan and W.I. Nayda, “Assessing Regional Impacts of Change: Linking Economic and Environmental Models,” *Agricultural Systems*, (63)3, 147-159, 2000.

Bansayat, P., L. Teeter, K. Flynn, and G. Lockaby, 1999. Relationships Between Landscape Characteristics and Nonpoint Source Pollution Inputs to Coastal Estuaries. *Environmental Management* 23 (4): 539–549

Basnyat, P., L. Teeter, B.G. Lockaby, K.M. Flynn. 2000. Land Use Characteristics and Water Quality: A Methodology for Valuing of Forested Buffers. *Environmental Management* 26 (2): 153–161

Bingham, T.H., T.R. Bondelid, B.M. Depro, R.C. Figueroa, A.B. Hauber, S.J. Unger, G.L. Van Houtven, and A. Stoddard. 2000. “A Benefits Assessment of the Water Pollution Control Programs Since 1972: Part 1, The Benefits of Point Source Controls for Conventional Pollutants in Rivers and Streams.” Final Report. Prepared for Mahesh Podar, U.S. EPA Office of Water. EPA 68-C6-0021. (http://www.epa.gov/waterscience/economics/assessment.pdf)

Bondelid, T.R. and A. Stoddard. 2000. “National Water Pollution Control Assessment Model (NWPCAM) Version 1.1.” Prepared for U.S. Environmental Protection Agency, Office of Policy, Economics and Innovation, Washington, DC.

Bondelid, T.R, R. Dodd. C. Spoerri, and A. Stoddard. 1999. “The Nutrients Version of the National Water Pollution Control Assessment Model. Prepared for U.S. EPA Office of Water, and Office of Policy, Economics and Innovation, Washington, DC.

Bowie, G.L., W.B. Mille, D.B. Poralla, C.L. Campbell, J.R. Pagenkopf, G.L. Rupp, K.M. Johnson, P.W.H. Chen, S.A. Gerini, and C.E. Chamberlin. 1985. *Rates, Constants and Kinetic Formulations in Surface Water Quality Modeling, Second Edition*. EPA-600/3-85/040. U.S. Environmental Protection Agency, Office of Research and Development, Environmental Research Laboratory, Athens, GA. June.

Carson, R. T., and R. C. Mitchell. 1993. "The Value of Clean Water: The Public's Willingness to Pay for Boatable, Fishable, Swimmable Quality Water." *Water Resources Research* 29(July): 2445-2454.

Chang, C.C., B.A. McCarl, J.W. Mjelde, and J.W. Richardson. 1992. "Sectoral Implications of Farm Program Modifications." *American Journal of Agricultural Economics* 74(1992):38-49.

Di Toro, D.M. 1986. A diagenetic oxygen equivalents model of sediment oxygen demand. In: Hatcher, K.J. (ed.). *Sediment Oxygen Demand, Processes, Modeling and Measurement*. Inst. Natural Resources, University of Georgia, Athens, GA. pp 171-208.

Di Toro, D.M., P.R. Paquin, K. Subburamu, and D.A. Gruber. 1990. Sediment oxygen demand model: Methane and ammonia oxidation. *American Society of Civil Engineers Journal of the Environmental Engineering Division*, 116(5):945-987.

Eidenshink, J.C. 1992. The 1990 conterminous U.S. AVHRR data set. Photogrammetric Engineering and Remote Sensing 58(6):809-813.

Energy Information Administration. 2002. 2001 Annual Energy Review. www.eia.doe.gov/emeu/aer/pdf/03842001.pdf

Gates and Associates, Inc. 1982. Estimation of Streamflows and the Reach File, Prepared for the U.S. Environmental Protection Agency, Monitoring Branch, Washington, DC.

Goolsby, Donald A., William A Battaglia, Gregory B. Lawrence, Richard S. Artz, Brent T. Aulenbach, Richard P. Hooper, Dennis R. Keeney, and Gary J. Stensland. 2000. "Hypoxia in the Gulf of Mexico: Progress towards the completion of an Integrated Assessment. Topic 3: Flux and sources of nutrients in the Mississippi-Atchafalaya River Basin" *NOAA National Center for Coastal Ocean Science.*

Greenhalgh, S. and Faeth, P. 2001. "A Potential Integrated Water Quality Strategy for the Mississippi River Basin and the Gulf of Mexico" In Optimizing Nitrogen Management in Food and Energy Production and Environmental Protection: Proceedings of the 2nd International Nitrogen Conference on Science and Policy. *The Scientific World* 1.

Henderson, F.M. 1966. *Open Channel Flow*. New York: Macmillian Publishing Co., Inc.

Hydroscience. 1972. *Addendum to Simplified Mathematical Modeling of Water Quality*. Prepared by Hydroscience, Inc., Westwood, NJ, for the U.S. Environmental Protection Agency, Water Quality Management Planning, Washington DC. May.

Hydroscience. 1971. *Simplified Mathematical Modeling of Water Quality*. Prepared by Hydroscience, Inc., Westwood, NJ, under subcontract to The Mitre Corporation for the U.S. Environmental Protection Agency, Water Quality Management Planning, Washington DC. March.

Little, K., T. Bondelid, and A. Miles. 2003. Methodologies for Sensitivity Analysis, Calibration, Validation, and Uncertainty Analysis of NWPCAM 2.1. Prepared for U.S. Environmental Protection Agency, Office of Policy, Economics and Innovation, Washington, DC. Final Report. Prepared for Mahesh Podar, U.S. EPA Office of Water. EPA 68-C-01-142.

Lovejoy, S.B., and B. Dunkelberg. 1990. *Water quality and agricultural policies in the 1990s: Interim report No. 3 for development of the SCS National Water Quality Model*. Purdue University, West Lafayette, IN.

Lovejoy, S.B. 1989. *Changes in cropland loadings to surface waters: Interim report No.1 for the development of the SCS National Water Quality Model*. Purdue University, West Lafayette, IN.

Matthews, S., O'Connor, R., and A.J. Plantinga. 2002. Quantifying the Impacts on Biodiversity of Policies for Carbon Sequestration in Forests. *Ecological Economics* 40(1):71-87.

McCarl, B.A., and U.A. Schneider. 2000. "Agriculture's Role in a Greenhouse Gas Emission Mitigation World: An Economic Perspective." *Review of Agricultural Economics* 22:134-59.

McCarl, B.A., and U.A. Schneider. 2001. "Greenhouse Gas Mitigation in U.S. Agriculture and Forestry." *Science* 21:2481-2482.

McClelland, N.I. 1974. "Water Quality Index Application in the Kansas River Basin." Prepared for U.S. Environmental Protection Agency—Region VII. EPA-907/9-74-001.

Miller, D., and A. Plantinga. 1999. Modeling Land Use Decisions with Aggregate Data. *American Journal of Agricultural Economics*. 81:180-194.

Parks, P.J., I.W. Hardie. 1995. Least-cost Forest Carbon Reserves: Cost-effective Subsidies tp Convert Marginal Agricultural Land to Forests. *Land Economics*. 71:122-136

Plantinga, A.J., and J. Wu. 2003. "Co-Benefits from Carbon Sequestration in Forests: Evaluating Reductions in Agricultural Externalities from an Afforestation Policy in Wisconsin." *Land Economics.*

Plantinga, A. 1996. The Effect of Agricultural Policies on Land Use and Environmental Quality. *American Journal of Agricultural Economics*. 78:1082-1091.

Plantinga, A, T. Mauldin. 2001. A Method for Estimating the Costs of CO_2 Mitigation Through Afforestation. *Climatic Change.* 49:21-40

Plantinga, A, T. Mauldin, D. Miller. 1999. An Econometric Analysis of the Costs of Sequestering Carbon in Forests. *American Journal of Agricultural Economics.* 81:812-824

Redfield, A.C., B.H. Ketchum, and F.A. Richards. 1963. The Influence of Organisms on The Composition of Seawater. In: *The Sea, Vol.2,* M.N. Hill (Ed.). Wiley-Interscience, New York, NY. pp. 26-77.

RTI. 2001. "The National Water Pollution Control Assessment Model (NWPCAM V2): Quality Review Process Report for NWPCAM 2 RF3 – Reach Routing, Hydrology, and Hydraulic Datasets. Prepared for U.S. EPA Office of Water, and Office of Policy, Economics and Innovation, Washington, DC.

RTI. 2000. "Estimation of National Surface Water Quality Benefits of Regulating Concentrated Animal Feeding Operations (CAFOs) Using the National Water Pollution Control Assessment Model (NWPCAM). Prepared for U.S. EPA Office of Water, Washington, DC. <http://www.epa.gov/ost/guide/cafo/economics.html#envir>.

Schneider, U.A. 2000. "Agricultural Sector Analysis on Greenhouse Gas Emission Mitigation in the US." PhD dissertation, Department of Agricultural Economics, Texas A&M University, December.

Sharpley, A. N. and J. R. Williams, eds. 1990. EPIC—Erosion/Productivity Impact Caculator: 1. Model Documentation. U.S. Dept. Agric. Tech. Bull. No. 1768.

Stavins, R. 1999. The Costs of Carbon Sequestration: A Revealed-preference Approach. *American Economic Review*. 89:994-1009

USDA (Department of Agriculture). 1997. Predicting Soil Erosion by Water: A Guide to Conservation Planning With the Revised Universal Soil Loss Equation (RUSLE). Agriculture Handbook No. 703.

USEPA (Environmental Protection Agency). 2001. "Environmental and Economic Benefit Analysis of Proposed Revisions to the National Pollutant Discharge Elimination System Regulation and the Effluent Guidelines for Concentrated Animal Feeding Operations" Office of Water Washington DC. EPA Report #821-R-01-002 http://www.epa.gov/ost/guide/cafo/pdf/CAFO_Benefits.pdf

USEPA (Environmental Protection Agency). 1997. *1996 Clean Water Needs Survey (CWNS), Conveyance, Treatment, and Control of Municipal Wastewater, Combined Sewer Overflows and Stormwater Runoff. Summaries of Technical Data*. EPA-832-R-97-003. Office of Water Program Operations. Washington, DC.

Van Houtven, G.L., T.R. Bondelid, M.C. Buckley and R.C. Figueroa. 1999b. "National Surface Water Toxics Study – Status Report on Model Development. Prepared for U.S. EPA Office of Water, and Office of Policy, Economics and Innovation, Washington, DC.

Vaughn, W.J., 1986. The Water Quality Ladder. Included as Appendix B in Mitchell, R.C., and R.T. Carson. 1986. The Use of Contingent Valuation Data for Benefit/Cost Analysis in Water Pollution Control. CR-810224-02. Prepared for U.S. Environmental Protection Agency, Office of Policy, Planning, and Evaluation. Washington, DC.

Watson, R.T., I.R. Noble, B. Bolin, N.H. Ravindranath, D.J. Verardo, and D.J. Dokken (eds). 2000. *Special Report on Land Use, Land Use Change, and Forestry*. Intergovernmental Panel on Climate Change, Geneva, Switzerland: Cambridge University Press.

Wear, D., M. Turner, and R. Naiman. 1998. Land Cover Along an Urban-Rural Gradient: Implications for Water Quality. *Ecological Applications*. 8(3):619-630.

Figure 1 Overview of Process for Linking ASMGHG and NWPCAM

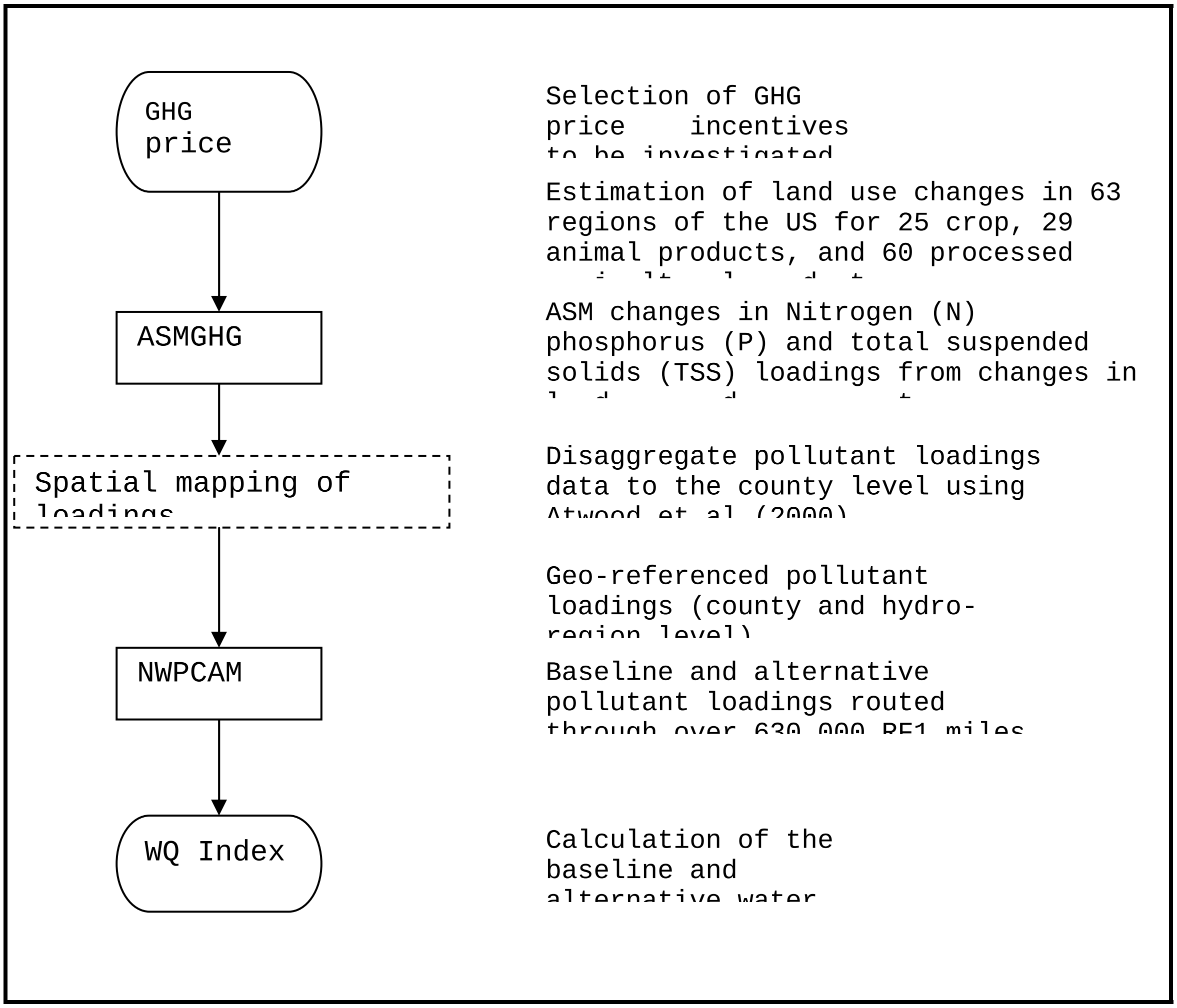

Figure 2 Changes in Water Quality Indices (WQI) by Reach: $25/Tonne Scenario Compared to Baseline

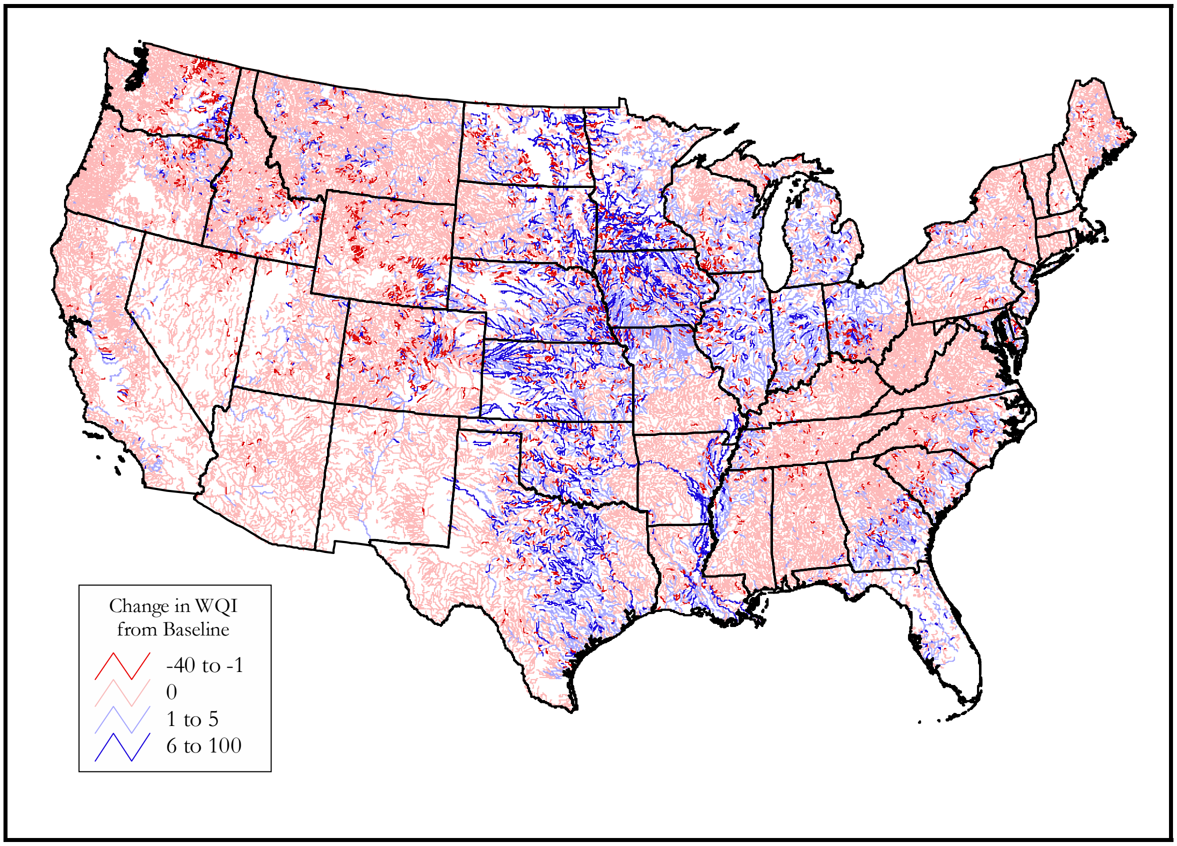

Note: Positive values represent improved water quality.

Table 1 National Summary of Welfare, Agricultural, and Environmental Impacts under Three GHG Prices

	Unit	Baseline $0/Tonne of CE	$25/Tonneof CE	$50/Tonneof CE
Welfare:				
U.S. producer welfare	billion $	30.93	31.84	36.73
U.S. consumer welfare	billion $	1183.15	1181.49	1177.5
Rest of the world welfare	billion $	256.64	256.15	255.37
Total social welfare (TSW)	billion $	1470.72	1469.48	1469.59
TSW less GHG payments	billion $	1470.72	1469.86	1467
Agricultural Activities:				
Crop production index	Base = 100	100	98.16	95.68
All goods production index (includes biofuels)	Base = 100	100	99.05	97.66
Crop price index	Base = 100	100	102.65	108.42
All goods price index	Base = 100	100	101.63	106.32
U.S. export sales	billion $	16	15.48	15.14
Land Use:				
Dry land	10^6 acres	240.78	240.65	227.01
Irrigated land	10^6 acres	60.21	56.18	58.15
Pasture land	10^6 acres	395.16	396.01	390.95
Afforestation	10^6 acres	0	5.8	12.52
Irrigation water use	10^6 acre-feet	73.08	67.39	68.2
Tillage Practices:				
Conventional	10^6 acres	203.32	68.93	54.08
Conservation	10^6 acres	84.96	27.72	11.65
No-till	10^6 acres	13.5	200.97	220.33
Environment:				
Nitrogen	10^6 acres	7.88	7.64	7.41
Phosphorus	10^6 acres	1.65	1.62	1.57
Potassium	10^6 acres	2.41	2.41	2.39
Pesticide	10^6 acres	7279.66	7345.05	6990.86
Erosion (TSS)	10^6 acres	3525.63	3541.66	3272.82
Greenhouse Gas:				
CH4	MMTCE	46.28	45.27	41.43
CO2	MMTCE	29.53	–57.48	–119.75
N2O	MMTCE	28.4	27.14	26.22
Total	MMTCE	104.2	14.93	–52.10

Table 2 Regional Water Quality Indices (WQI) Under the Baseline and Alternative GHG Pricing Scenarios

ASMGHG Region	Total Length of Reach System (Mi.)	Baseline WQI	Change in WQI	
			$25/Tonne of CE	$50/Tonne of CE
Northeast	45,082.80	74.16	0.12	0.02
Lake States	39,994.20	65.16	2.64	2.66
Corn Belt	64,636.20	57.64	2.57	2.55
North Plains	63,724.30	50.29	3.96	3.97
Appalachia	59,892.10	79.53	0.20	0.15
Southeast	45,107.50	80.90	0.57	0.67
Delta States	35,070.70	78.77	2.34	2.40
South Plains	62,293.30	55.39	2.96	3.12
Mountain	173,854.00	69.37	0.36	0.34
Pacific	73,426.50	76.59	0.25	0.21
Total U.S.	632,532.00	68.56	1.38	1.38

Note 1: Total length of miles of the ASMGHG regions is greater than the total miles because some reaches are in more than one region.
Note 2: Delta WQI values are scenario weighted sums minus baseline weighted sums, so positive values indicate water quality improvements.

Table 3 Regional Definitions

ASMGHG Region	States
Northeast	Connecticut, Delaware, Maine, Maryland, Massachusetts, New Hampshire, New Jersey, New York, Pennsylvania, Rhode Island, Vermont
Lake States	Michigan, Minnesota, Wisconsin
Corn Belt	Illinois, Indiana, Iowa, Missouri, Ohio
North Plains	Kansas, Nebraska, North Dakota, South Dakota
Appalachia	Kentucky, North Carolina, Tennessee, Virginia, West Virginia
Southeast	Alabama, Florida, Georgia, South Carolina
Delta States	Arkansas, Louisiana, Mississippi
South Plains	Oklahoma, Texas
Mountain	Arizona, Colorado, Idaho, Montana, Nevada, New Mexico, Utah, Wyoming
Pacific	California, Oregon, Washington

Table 4 GHG (Sum of CO_2, CH_4, and N_2O) Results from Cropland by Census Region in MMTCE

Region	Million Acres	Base	Actual Value		Absolute Change		Percentage Change	
			$25/Tonne of CE	**$50/Tonne of CE**	**$25/Tonne of CE**	**$50/Tonne of CE**	**$25/Tonne of CE**	**$50/Tonne of CE**
Northeast	11.09	1.61	0.40	0.26	–1.21	–1.35	–74.95	–83.74
Lake States	34.92	3.41	–4.88	–6.14	–8.29	–9.55	–242.96	–280.04
Corn Belt	85.50	16.47	–10.73	–12.70	–27.20	–29.17	–165.13	–177.13
North Plains	66.86	4.36	–6.74	–7.13	–11.10	–11.49	–254.54	–263.54
Appalachia	14.39	2.50	0.68	0.74	–1.82	–1.77	–72.85	–70.60
Southeast	9.44	0.67	–0.08	–0.16	–0.75	–0.83	–111.83	–124.24
Delta States	18.06	4.38	2.94	1.99	–1.44	–2.39	–32.79	–54.54
South Plains	28.03	4.48	–1.79	–1.62	–6.26	–6.10	–139.92	–136.24
Mountain	21.68	4.52	1.97	1.77	–2.55	–2.74	–56.47	–60.75
Pacific	11.03	4.88	2.60	2.41	–2.28	–2.47	–46.68	–50.59
Total U.S.	301.00	47.28	–15.62	–20.59	–62.90	–67.87	–133.03	–143.55

Table 5 N, P, and TSS Loadings (Million Tonnes) from Cropland by Region

Region	Million Acres	Base	Actual Value		Absolute Change		Percentage Change	
			$25/Tonne of CE	$50/Tonne of CE	$25/Tonne of CE	$50/Tonne of CE	$25/Tonne of CE	$50/Tonne of CE
TSS								
Northeast	11.09	176.05	177.06	145.82	1.02	–30.22	0.58	–17.17
Lake States	34.92	538.92	537.31	504.89	–1.60	–34.02	–0.30	–6.31
Corn Belt	85.50	1073.47	1047.32	1053.20	–26.16	–20.27	–2.44	–1.89
North Plains	66.86	420.33	420.83	407.70	0.50	–12.63	0.12	–3.00
Appalachia	14.39	201.07	183.73	214.14	–17.34	13.08	–8.62	6.50
Southeast	9.44	106.78	106.98	62.19	0.21	–44.59	0.19	–41.76
Delta States	18.06	591.15	638.28	471.27	47.13	–119.89	7.97	–20.28
South Plains	28.03	277.63	266.40	244.74	–11.23	–32.89	–4.04	–11.85
Mountain	21.68	85.37	83.40	82.38	–1.97	–3.00	–2.31	–3.51
Pacific	11.03	54.86	80.34	86.48	25.48	31.62	46.45	57.63
Total U.S.	301.00	3,525.63	3,541.66	3,272.82	16.03	–252.81	0.45	–7.17
Nitrogen								
Northeast	11.09	0.52	0.51	0.40	–0.01	–0.12	–1.94	–23.62
Lake States	34.92	0.76	0.76	0.72	–0.01	–0.04	–0.81	–5.36
Corn Belt	85.50	2.48	2.42	2.44	–0.06	–0.04	–2.36	–1.58
North Plains	66.86	0.78	0.78	0.85	0.00	0.07	0.44	8.76
Appalachia	14.39	0.63	0.63	0.74	0.00	0.11	0.13	18.14
Southeast	9.44	0.28	0.29	0.22	0.00	–0.06	1.26	–21.27
Delta States	18.06	0.52	0.49	0.39	–0.02	–0.12	–4.47	–23.65
South Plains	28.03	0.66	0.60	0.55	–0.05	–0.11	–8.15	–16.69
Mountain	21.68	0.96	0.87	0.82	–0.08	–0.14	–8.65	–14.14
Pacific	11.03	0.29	0.27	0.27	–0.02	–0.02	–5.30	–7.60
Total U.S.	301.00	7.88	7.64	7.41	–0.24	–0.47	–3.07	–5.98
Phosphorus								
Northeast	11.09	0.08	0.08	0.06	0.00	–0.02	–1.88	–23.91
Lake States	34.92	0.22	0.22	0.21	0.00	–0.01	0.40	–4.26
Corn Belt	85.50	0.50	0.50	0.50	0.00	0.00	–0.74	0.27
North Plains	66.86	0.23	0.24	0.24	0.00	0.01	2.01	3.90
Appalachia	14.39	0.09	0.09	0.11	0.00	0.02	–0.35	16.18
Southeast	9.44	0.06	0.06	0.05	0.00	–0.01	0.33	–20.74
Delta States	18.06	0.10	0.10	0.08	0.00	–0.02	–0.03	–19.28
South Plains	28.03	0.14	0.12	0.11	–0.02	–0.02	–12.62	–18.42
Mountain	21.68	0.13	0.12	0.12	–0.01	–0.02	–7.93	–13.42
Pacific	11.03	0.10	0.09	0.09	–0.01	–0.01	–5.10	–6.65
Total U.S.	301.00	1.65	1.62	1.57	–0.03	–0.09	–1.97	–5.15

Table 6 Reduction in Loadings (Tonnes per Year) to the Gulf of Mexico under Alternative GHG Pricing Scenarios

TSS		N	
$25/Tonne of CE	**$50/Tonne of CE**	**$25/Tonne of CE**	**$50/Tonne of CE**
8,783,098	9,557,527	144,565	160,578

Note: Values are reductions in tonnes/yr. A positive value is a reduction; a negative value is an increase.

Endnotes

---

[1]See for example Adams et al. (1993), Parks and Hardie (1995), Alig et al. (1997), Plantinga et al. (1999), Stavins (1999), Plantinga and Mauldin (2001).

[2] The 630,000 mile stream network is referred to as the Reach File 1.0 – or RF1 – level of resolution commonly used by the US Environmental Protection Agency and other federal and state agencies tracking water quality.

[3] All RTI reports are available upon request from corresponding author. Multiple applications and reviews of the NWPCAM model can be found on the EPA website by searching for NWPCAM (http://oaspub.epa.gov/webi/meta_first_new2.try_these_first).

[4]These reach files were designed by the US EPA Office of Water. Information on these and other national hydrologic information can be found at the following web-address—http://www.epa.gov/owowwtr1/monitoring/rf/rfindex.html

[5] NWPCAM can report results at the RF1 or RF3 level. Because RF3 is a sub-set of RF1, assigning each 1 km^2 land use cell to an RF3 reach thus also maps the cell to a RF1 reach.

[6] In the NWPCAM modeling framework loadings from the following loadings can be traced through the national river network; conventional pollutants (e.g. biochemical oxygen demand, total suspended solids, fecal coliform), nutrients (i.e. nitrogen, phosphorus), and toxic compounds (e.g. arsenic, cadmium).

[7]More information regarding the SPARROW model can be found at the following web address http://water.usgs.gov/nawqa/sparrow/

[8] New weights were calculated so that the ratios of the six remaining weights were retained and would still sum to one.

[9] 1 metric tonne = 1.1022 short tons

[10]Note, we do not factor in other sectors of the economy or non-US agricultural markets experiencing a C price.

[11]We were unable to map 5 of the approximately 3000 counties because of imperfect overlap of the two model databases, reflecting somewhat incomplete coverage.

[12] For example, if the carbon price introduced in ASMGHG results in a 5% reduction in N loadings in a specific county, the nitrogen loadings to all river reaches in that county will also be reduced by 5%. This reduction in N is then modeled through the national river network. It is beyond the scope of this report to provide further details concerning the full modeling processes and in-stream kinetics used in NWPCAM. More detail about NWPCAM (including an application) can be found online at: http://www.epa.gov/waterscience/economics/ and also at http://www.epa.gov/ost/guide/cafo/economics.html#envir

[13] Publicly available and reliable livestock and forestry pollutant data are not available to evaluate the impacts of their respective activities. Insufficient data and resources did not permit us to spatially disaggregate and model manure and forestry loadings. It is unclear whether the net result of including these loadings would increase or decrease water quality in the net.

[14] Note this decline in consumer welfare applies only to the change in agricultural consumption. Social benefits from a reduction in adverse impacts from climate change are not included in this calculation.

[15]The passage of the Federal Water Pollution Control Act of 1972 (FWPCA-72) established national water quality objectives and identified a number of goals in order to ensure the achievement of these objectives. Later amendments to the FWPCA-72 lead to the passage of the Clean Water Act of 1977 (CWA). Section 1251of the Clean Water Act defines the goal of establishing “boatable and fishable” water quality conditions in the nation’s waters by 1985. However, in the 1998 National Water Quality Inventory Report to Congress, it was reported that about 40 percent of the streams that were monitored by the EPA were not clean enough to be classified as fishable or swimmable.

[16] Although the range here is large, it was developed to capture all changes in WQI which included a few outliers at the extreme low end of this range. Most of the cases in which reach-level water quality declines show small reductions in WQI (less than 2 points).

[17] The changes in the two extremes of these ranges are composed mainly of outliers with large reductions or improvements in water quality. For the reaches predicted to have water quality decline, only 903 were predicted to fall by more than 1 point. A similar situation occurred for the improvements. In this range only 2,882 reaches improved by more than 6 points. The largest improvement was predicted to be 82 points.

[18] Because of the fine detail and small differences in WQI under alternative incentive pricing scenarios, only the national map of RF1 reaches for the $25/tonne is presented.

[19]These reductions in loadings account for nitrogen attenuation, or nitrogen loss in waterways in relation to channel width, by using streamflow-dependent first-order decay coefficients derived in the USGS SPARROW model.

[20]There may well be individual reaches and streams in the RF1 network that suffer water quality impairment.

[21] In our analysis we used Version 1.1 of the NWPCAM model. Thus, all references to NWPCAM in this appendix will be to Version 1.1.

[22] More information regarding the SPARROW model can be found at the following web address http://water.usgs.gov/nawqa/sparrow/